Star clusters: basic galactic building blocks
Proceedings IAU Symposium No. 266, 2009
R. de Grijs & J. R. D. Lépine, eds.

doi:10.1017/S1743921309991281

The globular cluster NGC 6642: evidence for a depleted mass function

Eduardo Balbinot, Basílio X. Santiago, Eduardo Bica and Charles Bonatto

Departamento de Astronomia, Universidade Federal do Rio Grande do Sul, Porto Alegre, Brazil
email: balbinot@if.ufrgs.br

Abstract. We present photometry for the globular cluster NGC 6642 using the F606W and F814W filters with the ACS/WFC third-generation camera aboard the *Hubble Space Telescope*. The colour–magnitude diagram shows sources reaching ≈ 6 mag below the turnoff in $m_{\rm F606W}$. Theoretical isochrone fitting was performed and evolutionary parameters were obtained, including the metallicity [Fe/H] $= -1.80 \pm 0.2$ dex and age, log(age/yr) $= 10.14 \pm 0.05$. We confirm that NGC 6642 is located in the Galactic bulge, at a distance of $d_{\odot} = 8.05 \pm 0.66$ kpc and suffers from a reddening of $E(B-V) = 0.46 \pm 0.02$ mag. These values are in general agreement with those of previous authors. Completeness-corrected luminosity and mass functions were obtained for different annuli centred on NGC 6642. Their spatial variation indicates the existence of mass segregation and depletion of low-mass stars. Most striking is the inverted shape of the mass function itself, with an increase in stellar numbers as a function of increasing mass. This has been observed previously in other globular clusters and is also the result of N-body simulations of stellar systems which have reached $\simeq 90\%$ of their lifetime and are subjected to strong tidal effects. We thus conclude that NGC 6642 is a very old, highly evolved globular cluster. Its current location close to perigalacticon, at only 1.4 kpc from the Galactic Centre, may contribute to this high level of dynamical evolution and stellar depletion.

Keywords. globular clusters: general, globular clusters: individual (NGC 6642), Galaxy: structure

1. Introduction

The bulge is known to host old but fairly metal-rich stellar populations, with high [α/Fe] ratios, indicating that it formed on a short timescale early in the Galactic history (Origlia *et al.* 2005). The bulge is thus an appropriate region to look for ancient GCs with distinct metallicities from those in the outer stellar halo. The bulge environment may also cause extreme dynamical evolution in star clusters due to bulge shocking and strong tidal effects (Aguilar *et al.* 1988; Shin *et al.* 2008).

Analyses of the structure and dynamical evolution of bulge GCs require high-resolution imaging to resolve individual stars in their cores and to effectively subtract contaminant field stars. The Advanced Camera for Surveys' Wide Field Channel (ACS/WFC) on board of the *Hubble Space Telescope (HST)* has provided a significant leap in the amount of such data on GCs, not only in the bulge, but also elsewhere (Sarajedini *et al.* 2007; Richer *et al.* 2008; Paust *et al.* 2009).

2. Data

NGC 6642 is projected towards the Galactic bulge, thus superimposed onto bulge and inner halo stellar populations. Dynamical studies of this GC, as well as other bulge

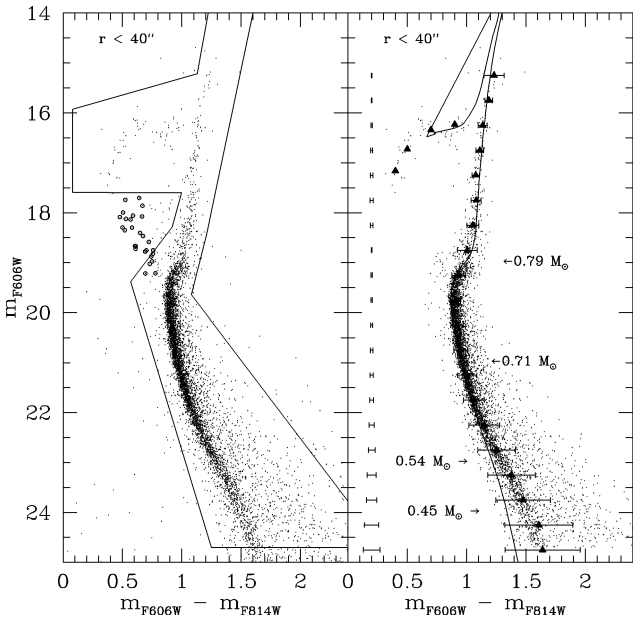

Figure 1. *(left)* CMD of all sources located within $r \leqslant 40''$ from the centre of NGC 6642. We also show the region used to select the cluster's evolutionary sequences. The blue-straggler candidates are marked with open circles. *(right)* Same CMD as in the left panel, but cut according to the selected region. The solid triangles show the CMD fiducial line and corresponding dispersion. The mean photometric error is shown in the extreme left of this panel. Some mass values are given along the main sequence. The best-fit isochrone is overplotted and has the following parameters: $\log(\text{age/yr}) = 10.14$, $[\text{Fe/H}] = -1.80$ dex, $E(B-V) = 0.46$ mag and $(m-M) = 14.55$ mag.

clusters, have been extremely difficult due to limitations of ground-based images. Here, we use *HST*/ACS data to overcome this difficulty.

The images were retrieved from the Space Telescope Science Institute (STScI)'s data archive (ID GO-9799) and were automatically reduced by the STScI pipeline. Two exposures were taken in the F606W and F814W filters, one short (10s) and one long (340s).

The photometry was done using the DOLPHOT software (Dolphin *et al.* 2000), which essentially uses *HST*-optimized PSF fitting. DOLPHOT was employed again in artificial-star mode. Based on fake-star experiments, we determined the completeness as a function of magnitude, colour and position. For more details on the photometry see Balbinot *et al.* (2009).

3. Colour–magnitude diagrams

Figure 1 shows the colour–magnitude diagram (CMD) for the stars located within $r \leqslant 40''$ ($\leqslant 1.6$ pc) from the nominal centre of NGC 6642. By restricting the image region, we strongly reduce field contamination.

We can see a well-defined structure in the main sequence (MS) spanning ~ 6 mag below the MS turnoff. The subgiant, red-giant and horizontal branches are also clearly seen. Some candidate asymptotic giant branch stars are also present. The solid contour in the left panel indicates our selected limits for these stellar evolutionary loci. The chosen limits also avoid effects of saturation and incompleteness. Open circles in the left panel indicate blue-straggler candidates.

https://doi.org/10.1017/S1743921309991281 Published online by Cambridge University Press

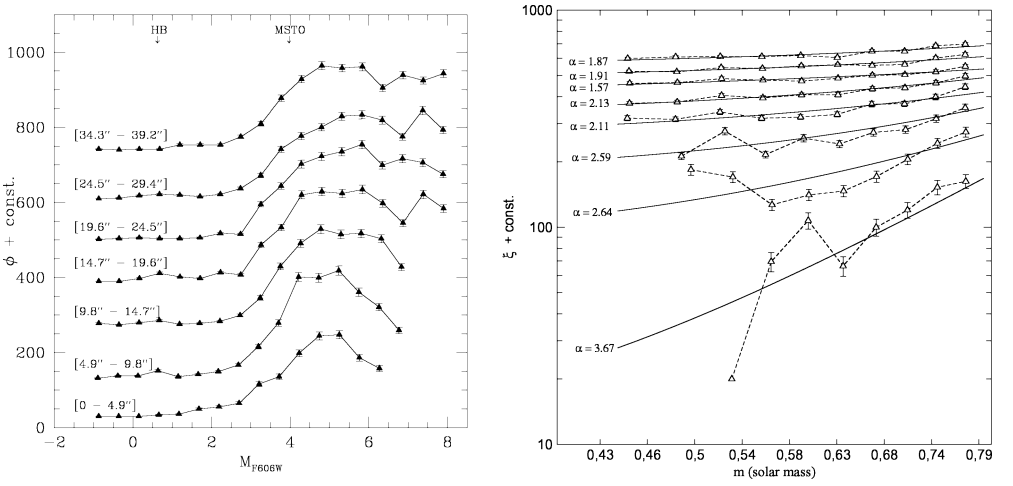

Figure 2. *(left)* Luminosity function of NGC 6642 stars at different radii, as indicated next to each curve. The positions of the MS turnoff (MSTO) and horizontal branch (HB) are indicated at the top. An offset was added to each curve to avoid overlap. In the inner regions, the completeness function falls off more rapidly as a function of magnitude, yielding a brighter cutoff limit. *(right)* Present-day mass functions (PDMFs) for different annuli around the centre of NGC 6642. Distance from cluster centre increases upwards. We use the same radial bins as in the left-hand panel. A constant offset was added to the star counts to avoid confusion. Fits to power-law PDMFs are also shown and the corresponding slopes given.

In the right panel of Figure 2, the GC fiducial line is shown on top of the selected stars. We also show the dispersion around the fiducial points plus the mean photometric error for each magnitude bin.

The NGC 6642 inner-field CMD is used to visually fit isochrones. We use the isochrone grid computed by Girardi *et al.* (2000) for that purpose. To determine parameter uncertainties and to test our visual fit, we generated model cluster fiducial lines and compared them with the observations using a simple algorithm described in Balbinot *et al.* (2009). The best-fit isochrone is shown in the right panel of Figure 2. The corresponding parameters are $\log(\text{age/yr}) = 10.14 \pm 0.05$ and $[\text{Fe/H}] = -1.80 \pm 0.2$ dex, $E(B-V) = 0.46 \pm 0.02$ mag and $(m-M) = 14.55 \pm 0.18$ mag.

4. Mass and luminosity functions

We now study the distribution of stars as a function of luminosity and mass. These are important tools to assess dynamical effects, such as mass segregation and stellar evaporation, that take place throughout a GC's lifetime.

Figure 2a shows the resulting luminosity functions (LFs) for different radial annuli. A 0.5 absolute-magnitude bin size was adopted. A constant offset was added to the curves to avoid cluttering. Poissonian error bars are also shown. Figure 2 includes evolved as well as MS stars. The most striking variation in the LF shapes occurs in the MS domain ($M_{\text{F606W}} > 3.5$ mag), where the LF is clearly depleted of low-luminosity stars and shows a clear peak in the inner cluster regions. In contrast, the outer regions display flatter LFs all the way to the detection limit.

Using the best-fit Padova isochrone, we convert absolute magnitudes to masses. Only stars below masses ~ 0.8 $M_\odot$ are considered, since according to the model, mass loss is more pronounced at higher masses. Figure 2b shows the resulting present-day mass function (PDMF).

https://doi.org/10.1017/S1743921309991281 Published online by Cambridge University Press

Mass segregation now stands out more clearly, as the PDMF is systematically steeper in the central regions of NGC 6642. More striking, however, is the fact that the number of stars decreases towards lower masses, in contrast to most observed PDMFs. Power laws were fitted to the data; the slopes are indicated in Figure 2b. The annuli are the same as in Figure 2a.

5. Conclusion

The CMD of NGC 6642 yields an age of 13.8 ± 1.6 Gyr and [Fe/H] $= -1.80 \pm 0.20$ dex. We also derived a colour excess of $E(B-V) = 0.46 \pm 0.02$ mag towards NGC 6642 and a distance comparable to that to the Galactic centre, $d_{\odot} = 8.05 \pm 0.66$ kpc. Given the direction of NGC 6642 on the sky, and assuming that the distance from the Sun to the Galactic centre is 8.0 kpc, we conclude that NGC 6642 currently occupies a very central position in the Galaxy, $d_{\rm GC} = 1.4$ kpc.

We point out that this inverted PDMF slope has also been observed in other recent studies (De Marchi & Pulone 2007; Paust *et al.* 2009). *N*-body GC simulations show that in tidal fields the preferential depletion of low-mass stars leads to a PDMF with inverted slope when the cluster has reached 90% or more of its associated dissolution time (Baumgardt & Makino 2003). The timescale associated with slope inversion is related to the time when the compact stellar remnants start to dominate the cluster mass. Since NGC 6642 is a very old GC that resides in a central region of the Galaxy, the shape of the PDMF can easily be understood in the context of tidal interactions. However, alternative explanations may be important, such as the gas-expusion model of Marks *et al.* (2009).

We thus conclude from an independent perspective that NGC 6642 is a very old, highly evolved, core-collapsed globular cluster.

References

Aguilar, L., Hut, P., & Ostriker, J. 1988, *ApJ*, 335, 720
Balbinot, E., Santiago, B., Bica, E., & Bonatto C. 2009, *MNRAS*, 396, 1596
Baumgardt, H. & Makino, J. 2003, *MNRAS*, 340, 227
De Marchi, G. & Pulone, L. 2007, *A&A*, 467, 107
Dolphin, A. E. 2000, *PASP*, 112, 1383
Girardi, L., Bressan, A., Bertelli, G., & Chiosi, C. 2000, *A&AS*, 141, 371
Marks, M., Kroupa, P., & Baumgardt, H. 2008, *MNRAS*, 386, 2047
Paust, N., *et al.* 2009, *AJ*, 137, 246.
Origlia, L., Valenti, E., Rich, R., & Ferraro, F. 2005, *MNRAS*, 363, 897
Richer, H., *et al.* 2008, *AJ*, 135, 2141
Sarajedini, A., *et al.* 2007, *AJ*, 133, 1658
Shin, J., Kim, S., & Takahashi, K. 2008, *MNRAS* (Letters), 386, L67

https://doi.org/10.1017/S1743921309991281 Published online by Cambridge University Press